In both cases deviations from a simple exponential time law are expected both for the decay of $Ru(bpy)_3^{3+}$ and the formation of H^+. Indeed at lower catalyst concentration the kinetic events appear to be biphasic, an initial fast period being followed by a slower component.[22] Only a single exponential is observed at TiO_2/RuO_2 concentrations of at least 200 mg/L.

Conclusion

The present study illustrates the advantage of coupling flash photolytic absorbance and conductance techniques for the study of water decomposition processes. The combination of these techniques proved to be a powerful tool to probe mechanistic details of light-induced oxygen generation mediated by colloidal redox catalysts. Application to the investigation of hydrogen generation is straightforward and presently undertaken.

The extraordinary high activity of colloidal TiO_2 particles charged with ultrafine deposits of RuO_2 has been unequivocally demonstrated. At relatively small RuO_2 concentrations rates for oxygen evolution are in the submillisecond time domain. Such a performance is required in cyclic water decomposition systems. It is comparable to the rate of water oxidation by the water splitting enzyme in photosystem II. However, in the latter case, the mechanism operative consists in the storage of redox equivalents after flash excitation. Only upon repeated exposure to light flashes are protons and oxygen liberated. This contrasts to the mode of intervention of the RuO_2 particles where charging and discharging occur simultaneously. This catalyst is presently being further improved to increase its efficiency in cyclic water decomposition systems.

Acknowledgment. This work was supported by the Swiss National Science Foundation, Ciba Geigy, and the United States Army Procurement Agency Europe.

Registry No. TiO_2, 13463-67-7; RuO_2, 12036-10-1; H_2O, 7732-18-5; O_2, 7782-44-7; $Ru(bpy)_3^{3+}$, 18955-01-6; $Ru(bpy)_3^{2+}$, 15158-62-0; $S_2O_8^{2-}$, 15092-81-6.

(21) Pulse radiolysis studies in our institute have shown that Pt sols can be precipitated by reduced viologens (V^+) at high V^+/Pt ratios.

(22) The slower component was used to evaluate k_7. In support of our explanation for the unusual dependenc of k_7 on the catalyst concentration, we found that the value of k_7 increases when the initial $Ru(bpy)_3^{3+}$ concentration produced by the laser pulse was decreased. Thus at 150 mg of TiO_2/L (2% of RuO_2) and $Ru(bpy)_3^{3+} = 2.5 \times 10^{-6}$ M the k_7 value is 4 times larger than with $Ru(bpy)_3^{3+} = 3.6 \times 10^{-6}$ M.

Temporary Anion States of Phosphabenzene, Arsabenzene, and Stibabenzene. Trends in the π and π^* Orbital Energies

P. D. Burrow,* A. J. Ashe, III,* D. J. Bellville, and K. D. Jordan*,†

Contribution from the Department of Physics and Astronomy, University of Nebraska, Lincoln, Nebraska 68588, Department of Chemistry, University of Michigan, Ann Arbor, Michigan 48109, and Department of Chemistry, University of Pittsburgh, Pittsburgh, Pennylsvania 15260. *Received February 27, 1981*

Abstract: Electron transmission spectroscopy is employed to study temporary negative ion formation in phosphabenzene, arsabenzene, and stibabenzene in the gas phase. From such measurements, we derive the electron affinities associated with the unstable anionic states of these molecules. The trends in the π^* electron affinities, including previously measured values for benzene and pyridine, are compared with those in the ionization potentials, and interpreted in light of the variations in carbon–heteroatom bond lengths and heteroatom electronegativities. The ground anionic states of the title compounds are found to be stable and thus inaccessible by electron impact. Estimates for the energies of these states are made based on the measured trends in the EA's and IP's. Anion states in addition to those associated with occupation of the π^* orbitals are also observed and possible designations are discussed.

The group 5 heterobenzenes, pyridine (II), phosphabenzene[1] (III), arsabenzene[1] (IV), stibabenzene[2a] (V), and bismabenzene[2b] (VI) form a unique series in which elements down an entire column of the periodic table have been incorporated into aromatic rings. Trends in the energy levels of such a series of closely related compounds can frequently be correlated with the systematic variation of molecular properties. A variety of techniques, both

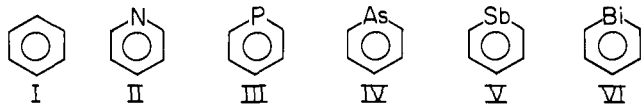

I II III IV V VI

spectroscopic and chemical, have been employed in such studies. Photoelectron spectroscopy, in particular, has been used to determine the ionization potentials (IP's), which may be correlated with the energies of the occupied molecular orbitals, within the context of the Koopmans' theorem approximation.

Data relating to the normally unfilled orbitals are equally desirable. The frontier molecular orbital theories of chemical reactivity, for example, utilize the energies of the lowest unoccupied molecular orbitals as well as those of the highest occupied molecular orbitals. Invoking Koopmans' theorem again, the energies of the unfilled orbitals can be associated with the measured electron affinities (EA's). In the gas phase, all of the anion states of I and II lie energetically above the ground state of the neutral molecule. Once formed, these temporary anion states undergo electron detachment in times typically of 10^{-13}–10^{-15} s. With the advent of electron scattering techniques, particularly electron transmission spectroscopy[3] (ETS), methods are now available for the study of such anion states. Using ETS, temporary anions are observed as sharp variations in the total scattering cross section as a function of electron impact energy. From such data the electron affinity may be determined, as well as information re-

* Address correspondence as follows: University of Nebraska, P.D.B.; University of Michigan, A.J.A. and D.J.B.; University of Pittsburgh, K.D.J.

† Camille and Henry Dreyfus Teacher–Scholar.

(1) Ashe, A. J. III *J. Am. Chem. Soc.* **1971**, *93*, 3293.

(2) (a) Ashe, A. J., III *J. Am. Chem. Soc.* **1971**, *93*, 6690. (b) Ashe, A. J., III; Gordon, M. D. *Ibid.* **1972**, *94*, 7596. Ashe, A. J., III *Tetrahedron Lett.* **1976**, 415.

(3) Sanche, L.; Schulz, G. J. *Phys. Rev. A* **1972**, *5*, 1672.

0002-7863/82/1504-0425$01.25/0

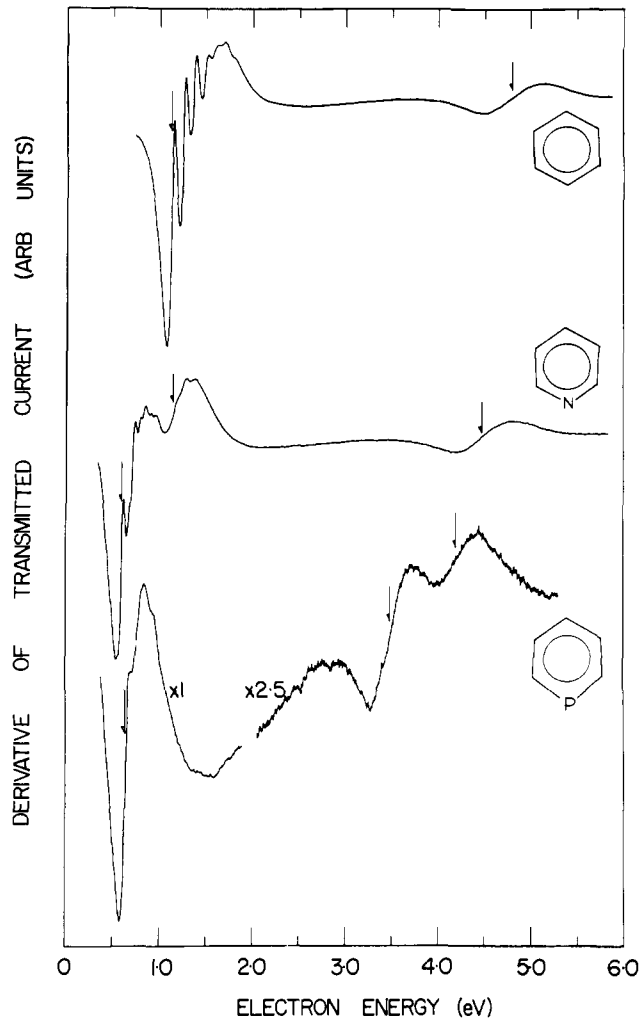

Figure 1. The derivative of transmitted current as a function of electron energy in benzene, pyridine, and phosphabenzene. The arrows mark the most probable attachment energy for each anion state.

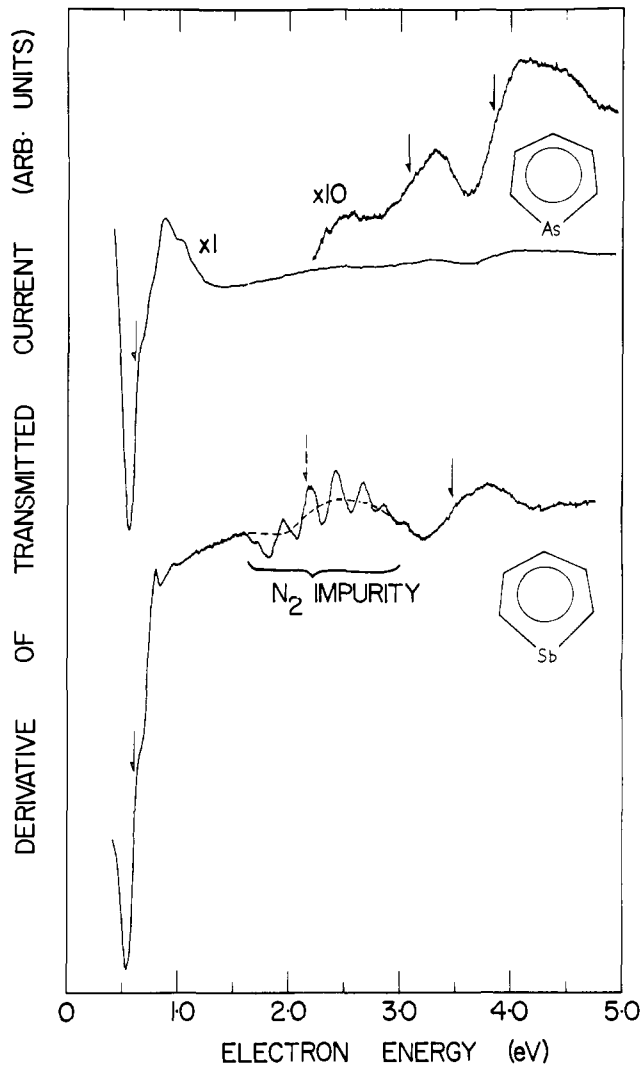

Figure 2. The derivative of transmitted current as a function of electron energy in arsabenzene and stibabenzene.

garding the anion potential surface and vibrational modes, if the lifetime of the anion is sufficient to permit nuclear motion. A more thorough discussion of ETS has been given by Schulz and co-workers,[3-5] and a review of the application of this technique to hydrocarbon molecules has recently been published.[6]

Apparatus

The data we present here were acquired on an electron transmission apparatus similar to that described by Sanche and Schulz,[3] although the dimensions of certain apertures have been changed to improve the transmission characteristics. In addition, the electrodes are constructed of molybdenum rather than a gold-plated copper–nickel alloy. The modulation technique introduced by Sanche and Schulz[3] is employed to obtain the derivative with respect to energy of the electron current transmitted through a cell containing the gas as a function of the impact energy. As used in a variety of spectroscopies, the derivative technique enhances the rapidly varying structures in the signal. The energy scales are calibrated in a gas admixture with He by reference[3] to the $(1s2s^2)$ ^2S state of He^-.

Results

In Figures 1 and 2, we present the electron transmission spectra of compounds I–V. The new data on phospha-, arsa-, and stibabenzene were taken with small samples and it was not possible to achieve the high signal-to-noise ratios shown for benzene and pyridine. During the course of the runs, the gas pressure could not be completely stabilized, and therefore the relative size of the resonances in a given compound may not be accurate. Finally, we should note that the final steps in the synthesis of stibabenzene were carried out in a vessel attached to the gas inlet line and the product was distilled directly into the collision chamber. A small nitrogen impurity led to the oscillatory structure present in the 2–3 eV region. We have drawn a dashed line through this structure to indicate the approximate signal in the absence of N_2.

The benzene transmission spectrum has been previously published by a number of workers[4,5,7,8] and that of pyridine by Nenner and Schulz.[5] Our spectra shown in Figure 1 are in good general agreement with respect to the number of sharp features; the overall resonance profiles however are somewhat altered from previous versions because of the improved discrimination in the present apparatus against electrons scattered at small angles. A more detailed discussion of this aspect will be given elsewhere. We note also that our preferred value for the lower benzene anion attachment energy is decreased by 0.03 eV, and that of the upper anion by 0.05 eV from values reported earlier.[7] The new values remain within the previous error limits, but we believe them to be more accurate. For pyridine, our values for the lower two anion states fall within 0.04 eV of those given by Nenner and Schulz.[5] Our energy for the third anion state however is 0.1 eV lower.

First, we review briefly the interpretation of the spectra. The structure appearing near 1.12 eV in the benzene spectrum is due

(4) Sanche, L.; Schulz, G. J. *J. Chem. Phys.* **1973**, *58*, 479.
(5) Nenner, I.; Schulz, G. J. *J. Chem. Phys.* **1975**, *62*, 1747.
(6) Jordan, K. D.; Burrow, P. D. *Acc. Chem. Res.* **1978**, *11*, 341. A bibliography of ETS papers is available from one of the authors (P.D.B.).
(7) Jordan, K. D.; Michejda, J. A.; Burrow, P. D. *J. Am. Chem. Soc.* **1976**, *98*, 1295. Jordan, K. D.; Michejda, J. A.; Burrow, P. D. *Ibid.* **1976**, *98*, 7189.
(8) Frazier, J. R.; Christophorou, L. G.; Carter, J. G.; Schweinler, H. C. *J. Chem. Phys.* **1978**, *69*, 3807.

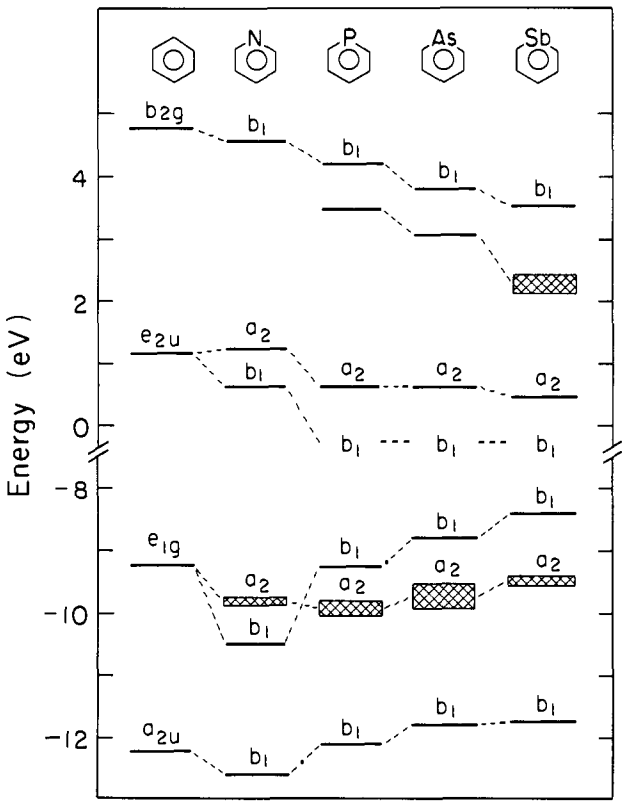

Figure 3. Correlation diagram using the experimental EA's and IP's of benzene and the group 5 heterobenzenes. The IP's are from ref 18.

to the $^2E_{2u}$ ground state anion which is sufficiently long lived that it displays sharp vibrational structure in the symmetric breathing mode.[3] An arrow marks the energy of the midpoint between the derivative extrema associated with the first, and largest, of the vibrational features. We therefore associate this point with both the adiabatic and vertical attachment energies, that is, with -EA. The structure centered at 4.8 eV results from temporary occupation of the $b_{2g}(\pi^*)$ orbital. As no vibrational structure is present, the adiabatic attachment energy cannot be located; the arrow marks the vertical or most probable value. Similar conventions are employed in the remaining spectra.

In the heterobenzenes the degenerate $^2E_{2u}$ anion is split, giving rise to $^2B_1$ and $^2A_2$ states. For pyridine, this splitting was first observed by Huebner et al.[9] using the electron scavenger method, and later by Nenner and Schulz[5] in the electron transmission spectrum. In contrast to pyridine, our spectra for phospha-, arsa-, and stibabenzene shown in Figures 1 and 2 indicate only a single anion state below 1.5 eV. However, a new feature is now present in the upper portion of the spectra of each of these three compounds.

A correlation diagram showing the measured IP's and EA's for compounds I–V is given in Figure 3. Our suggested designations for the anion states are also indicated. At the simplest level, these assignments are based on the monotonic trend in the upper b_1 level in II–V and the expected relative insensitivity of the $a_2(\pi^*)$ orbitals to heteroatom substitution, a property reflected also in the filled a_2 orbitals. The absence in III–V of a $^2B_1$ (π^*) state correlating to the degenerate $^2E_{2u}$ level in the benzene anion is also consistent with our assignment. If the stabilizing trend displayed by the upper $b_1(\pi^*)$ orbital also occurs for the lower $b_1(\pi^*)$ orbital, the ground state anion will appear below 0 eV where it is inaccessible to formation by electron impact. This interpretation is discussed in more detail later in the paper. Here we note that it is consistent with the findings of ESR studies[10]

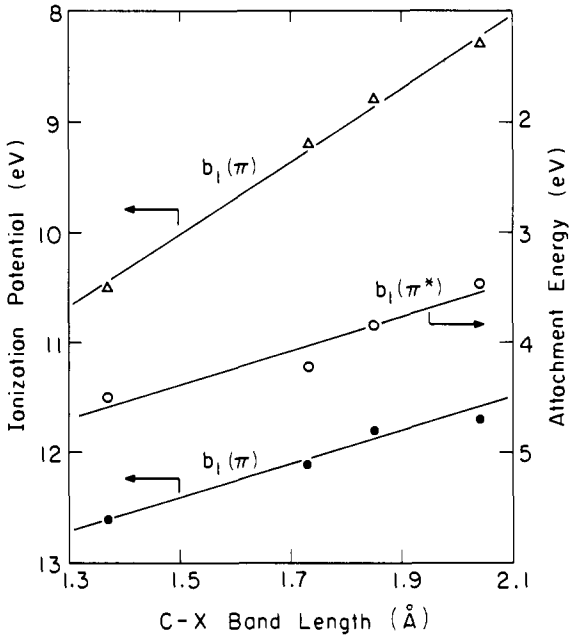

Figure 4. Ionization potentials and attachment energies (-EA) of the heterobenzenes as a function of C–X bond length. The scale for the IP's is on the left. The scale for -EA is on the right.

in solution that the ground state of the phosphabenzene anion is $^2B_1$, and with ab initio calculations[11] for phosphabenzene which predict that the $b_1(\pi^*)$ orbital lies below the $a_2(\pi^*)$ orbital.

Discussion

In this section we examine the correlations among the IP's, EA's, and other molecular properties, and provide additional support for our assignments. We then discuss our findings and those of other workers for the IP's in terms of simple Hückel molecular orbital (HMO) theory.

It is apparent from Figure 3 that electronegativity considerations alone are unable to explain the observed trend in both the IP's and EA's, necessitating the examination of the role played by other factors. In view of the large geometry changes along this series of compounds, for example, molecules II–V have C–X bond lengths of 1.37, 1.73, 1.85, and 2.05 Å, respectively, we consider the implications of these changes for the molecular orbitals. As the C–X bond lengths increase, one expects, from overlap considerations, a parallel *destabilization* of the $b_1(\pi)$ orbitals and *stabilization* of the $b_1(\pi^*)$ orbitals along the series II–V. This is precisely what is observed experimentally for the nominally -12 eV $b_1(\pi)$ and 4 eV $b_1(\pi^*)$ orbitals.

The dependence on bond length is seen more clearly in Figure 4 where we plot the IP's and EA's associated with the $b_1(\pi)$ and $b_1(\pi^*)$ orbitals vs. the C–X bond length for the various heterobenzenes. The energy scale for the filled b_1 orbitals is to the left of the figure, that for the second $b_1(\pi^*)$ to the right. Each of the three lines displays a nearly linear dependence on bond length. Perfectly linear behavior is not expected since the overlap between orbitals on different atoms is actually exponential, and since the bond angles also vary considerably. Within experimental errors the slopes for the second b_1 IP and second b_1 EA coincide, justifying our earlier statement that the destabilization of one orbital is paralleled by an associated stabilization of the other. It should be mentioned here that the anion state associated with the $b_1(\pi^*)$

(9) Huebner, R. H.; Compton, R. N.; Schweinler, H. C. *Chem. Phys. Lett.* **1968**, *2*, 407.
(10) Gerson, F.; Plattner, G.; Ashe, A. J., III; Maerkl, G. *Mol. Phys.* **1974**, *28*, 601.
(11) von Niessen, W.; Dierksen, G. H. F.; Cederbaum, L. S. *Chem. Phys.* **1975**, *10*, 345.
(12) Ashe, A. J., III *Acc. Chem. Res.* **1978**, *11*, 153.
(13) The values of the C–X bond lengths can be found in the following papers. C–N: Sorensen, G. O.; Mahler, L.; Rastrup-Andersen, N. *J. Mol. Struct.* **1974**, *20*, 119. C–P: Wong, T. C.; Bartell, L. S. *J. Chem. Phys.* **1974**, *61*, 2840. C–As: Wong, T. C.; Bartell, L. S. *J. Mol. Struct.* **1978**, *44*, 169. C–Sb: Fong, G. D.; Kuczkowski, R. L.; Ashe, A. J., III *J. Mol. Spectrosc.* **1978**, *70*, 197.

Table I. Vertical π-Electron Affinities and Ionization Potentials of Benzene, Pyridine, Phosphabenzene, Arsabenzene, Stibabenzene, and Bismabenzene[a]

molecule	exptl IP's, eV			exptl EA's, eV			estimated EA's, eV
	π_1	π_2	π_3	π_1^*	π_2^*	π_3^*	π_1^*
benzene	9.25 (e_1g)	9.25 (e_1g)	12.20 (a_{2u})	−1.12 (e_{2u})	−1.12 (e_{2u})	−4.80 (b_{2g})	
pyridine	9.7–9.8 (a_2)	10.5 (b_1)	12.6 (b_1)	−0.59 (b_1)	−1.16 (a_2)	−4.48 (b_1)	
phosphabenzene	9.2 (b_1)	9.8–10.0 (a_2)	12.1 (b_1)	>0 (b_1)	−0.64 (a_2)	−4.21 (b_1)	0.7
arsabenzene	8.8 (b_1)	9.6–9.9 (a_2)	11.8 (b_1)	>0 (b_1)	−0.62 (a_2)	−3.84 (b_1)	1.1
stibabenzene	8.3 (b_1)	9.4–9.6 (a_2)	11.7 (b_1)	>0 (b_1)	−0.60 (a_2)	−3.47 (b_1)	1.6
bismabenzene	7.9 (b_1)	9.2–9.6 (a_2)					2.0

[a] The ionization potentials are from Batich et al. (ref 18) and Bastide et al. (ref 18).

orbital of phosphabenzene is partially overlapped by the strong feature at 3.51 eV, discussed below. This tends to increase the apparent attachment energy for this state and accounts in part for the shift of this point from the straight line drawn in Figure 4.

If we assume that the most important factor for determining the relative orbital energies is the variation in the C–X orbital overlaps, then the same "reflection" symmetry should also apply to the other b_1 orbital pair, that is, the $b_1(\pi^*)$ correlating to $e_{2u}(\pi^*)$ and $b_1(\pi)$ correlating to $e_{1g}(\pi)$. The low-lying anions of phospha-, arsa-, and stibabenzene are then predicted to be stable, lying below 0 eV in the gas phase. It is then apparent why the transmission spectra show only one state below 1.5 eV in these species.

Stable negative ions cannot be studied by electron scattering methods but are amenable to investigation by a variety of other techniques. In the absence of such data we can roughly estimate the EA's for the heavier compounds from the trends evident in Figure 4. Assuming that the energies of the low-lying unfilled $b_1(\pi^*)$ orbitals do, in fact, exactly mirror those in the high-lying occupied $b_1(\pi)$ orbitals as a function of bond length, and anchoring the line on our experimental value for the first $^2B_1$ anion of pyridine, we find first EA's of 0.7, 1.1, 1.6, and 2.0 eV for phospha-, arsa-, stiba-, and bismabenzene, respectively. Because of the nature of the assumptions in this treatment, the error in these EA's is difficult to ascertain. However, it can be argued that these values represent upper bounds to the true EA's. This point deserves brief elaboration. In a simple one-electron picture, the matching slopes of the lower two curves in Figure 4 imply that the electronegativity differences along the series II–V play a negligible role in determining the IP's and EA's. One cannot, however, rule out the possibility that the anion state associated with electron capture into the second $b_1(\pi^*)$ orbital contains a small admixture of a higher lying doubly-excited configuration of the same symmetry. These latter states would certainly shift to lower energy in going from II through V causing a stabilizing trend in the EA's which opposes that expected from electronegativity differences. The excellent agreement in slopes in Figure 4 may therefore result from cancellation of these effects. Failure to compensate for the electronegativity changes in extrapolating the first EA's would cause them to be too large. The experimental IP's and EA's, together with the estimated first EA's, are summarized in Table I.

In the preceding discussion we have focused our attention on the b_1 π and π^* orbitals. It remains to discuss the trends in the a_2 π and π^* orbitals and the presence of the additional anion states shown in Figures 2 and 3 in the 2.2–3.5 eV range for the P, As, and Sb compounds.

We expect little variation in the energies of the $^2A_2$ states of either the cations or the anions with C–X bond length changes alone because of the node located at the X atom. In fact, the $^2A_2$ anions of compounds III–V are about 0.6–0.7 eV more stable than that of pyridine. A portion of this stabilization could arise from increases in the separation between carbon atoms adjacent to the heteroatom, that is, the C_1–C_5 spacing. These distances are 2.406, 2.356, 2.670, 2.771, and 2.950 Å for I–V. A simple orbital picture however would lead one to expect similar shifts in both π and π^* orbitals, whereas the photoelectron data indicate that the $a_2(\pi)$ orbitals are slightly destabilized in progressing from II through V. However, it should be noted that there is an essential difference in the nature of the anion and cation wave functions not accounted for in the simple orbital picture. The former will be much more diffuse and effects due to changes in overlap between two widely spaced atoms, such as C_1–C_5, may thus be more pronounced in the anion than in the cation.

Inductive effects will tend to destabilize both the a_2 π and π^* orbitals of III–V relative to those of II. The overlap and inductive effects combined may explain why the a_2 π orbital is relatively unshifted in energy and, allowing for the more diffuse nature of the anion, could also account for the stabilization in the anion energies. Nevertheless, it is not compelling that overlap changes account fully for the stabilization of the $a_2(\pi^*)$ orbitals in III–V with respect to II. We return to a second possible mechanism following a discussion of the additional anion state observed in III–V.

There are two possible classifications for the additional anion states observed at 3.51, 3.07, and 2.2 eV in compounds III–V, respectively. First, the state could be a core-excited anion state, or "Feshbach" resonance,[14] in which an electron is promoted from a filled $a_2(\pi)$ or a lone pair (n) orbital to a low-lying π^* orbital together with the capture of the incident electron into the same π^* orbital. Experience with other atomic and molecular systems has indicated that such anions are usually found near the threshold for producing the associated excited state of the neutral molecule.[14] Excited states based on lone pair promotions, $n \rightarrow \pi^*$, for pyridine, phosphabenzene, and arsabenzene have been associated[1] with transitions at 4.8, 3.5, and 3.3 eV, respectively. Feshbach resonances associated with these states in phosphabenzene and arsabenzene would therefore lie near the energies of the additional features in the transmission spectra. In pyridine it could be argued that the resonance associated with the 4.8 eV transition is obscured by the 4.45 eV anion state. Attractive as this agreement is, we do not favor this interpretation. There is little precedent in simpler molecules for such valence excited Feshbach resonances to appear prominently in the transmission spectrum.[15]

The second and more likely assignment attributes the new features to filling of low-lying σ^* orbitals. There is now ample evidence for such resonances in other hydrocarbons which incorporate elements from the second row of the periodic table. Recent work in the chloroethylenes,[16] for example, reveals low-lying features in addition to those attributed to filling of π^* orbitals. Ab initio calculations in these systems support a σ^* assignment for these resonances. Similar features also appear in saturated hydrocarbons upon chlorine substitution.[17]

We have carried out ab initio SCF calculations employing double-ζ basis sets in pyridine and phosphabenzene which also support this assignment. The first σ^* orbital of phosphabenzene is found to be of b_2 symmetry and to display a substantially different character than the corresponding orbital of pyridine; in particular, it lies at lower energy and is much more localized on the heteroatom. There is also the possibility that the new features are due to σ^* orbitals with an appreciable contribution from a "d" orbital on the heteroatom. However we expect these to lie

(14) See, for example: Schulz, G. J. *Rev. Mod. Phys.* **1973**, *45*, 378, 423.
(15) Feshbach resonances with the excited electrons in Rydberg orbitals, on the other hand, are well established and highly visible using ETS.
(16) Burrow, P. D.; Modelli, A.; Chiu, N. S.; Jordan, K. D. *Chem. Phys. Lett.* **1981**, 270.
(17) Burrow, P. D.; Modelli, A.; Chiu, N. S.; Jordan, K. D., unpublished.

higher in energy than the b_2 σ^* orbital.

A definitive assignment for the additional features in the electron transmission spectra of compounds III–V cannot be made at this time, although our preference is argued above. Additional guidance would be provided by more detailed calculations and by further ETS work on other molecules incorporating the same heteroatoms. Electron scattering experiments in which the angular dependence is measured would yield direct information about the symmetries of the observed anion states.

Returning now to the unexpectedly large stabilization of the $^2A_2$ anions in III–V, a second mechanism involving the mixing between two configurations of A_2 symmetry is now evident. The higher interacting state need not, of course, be the one apparent in the transmission spectrum. Possible $^2A_2$ excited states include a Feshbach resonance, as discussed earlier, in the $[a_2(\pi)^{-1}b_1(\pi^*)^2]$ configuration, or a resonance involving the a_2 component of a d orbital on the heteroatom. Again, with only the experimental data at hand, the dominant interaction cannot be specified. The mechanism however is clearly viable.

We turn now to a discussion of the conclusions previously drawn from the photoelectron spectra alone and examine their consistency with the additional data available from ETS. Photoelectron spectroscopy reveals that the $e_{1g}(\pi)$ orbital is split by more than 0.5 eV in all the heterobenzenes. While in pyridine the first π IP is attributed to the a_2 orbital, for compounds III–V it has been assigned to the b_1 orbital.[18,19] This reversal of the cation states has been explained by noting that the nitrogen atom in pyridine is net electron withdrawing while the heavier heteroatoms are net electron donating.[11,18,19] However, as noted in our earlier discussion, this interpretation is inconsistent with the trends observed in the EA's; if this were the most important factor responsible for the difference in the relative ordering of the pyridine orbitals from that in the other heterobenzenes, then the $b_1(\pi^*)$ orbitals of compounds III–V would be *less* stable than the corresponding orbitals of pyridine. Exactly the reverse is observed.

Batich et al.[18] found that the IP's of the highest $b_1(\pi)$ orbitals varied linearly with the IP's of the free heteroatoms, X = N, P, As, Sb, and Bi, and that to very good approximation:

$$IP[b_1(\pi)] = 5.24 \text{ eV} + 0.362IP(X) \quad (1)$$

Similarly for ionization from the second $b_1(\pi)$ orbital they found

$$IP[b_1(\pi)] = 10.25 \text{ eV} + 0.163IP(X) \quad (2)$$

The slopes in these two expressions are very close to those, $^1/_3$ and $^1/_6$, expected from simple HMO theory.

In Figure 4 we demonstrated that one also could obtain good fits of the b_1 IP's to the C–X bond lengths of the heterobenzenes. In fact, these two pictures are related. The increase in the C–X bond length along the series N, P, As, Sb, Bi corresponds closely to the increasing size of the X atom. It is also well known that the IP's generally decrease as one proceeds down a column of the periodic table: the larger the atom, the easier it is to remove an electron from the outermost electron shell or subshell. Hence, it is not surprising that the $b_1(\pi)$ IP's of the heterobenzenes are well correlated with either the IP's of the heteroatoms or with the C–X bond lengths.

In terms of simple Hückel theory, the picture employed by Batich et al. to explain trends in the IP's focused on variations in the diagonal coulomb terms (α_X). However, as may be seen from the correlation diagram, Figure 3, the variations in both coulomb and resonance interactions (β_{CX}) are necessary to explain the shifts in both the filled and unfilled orbitals in the entire series I–V. In particular it is necessary to assume that β_{CX} decreases in magnitude along the series. Both terms are important in explaining the relative spectra of benzene and pyridine, with the change in the coulomb integral predominating. However, the trends along II–V are consistent with the greater importance of the variation in the resonance interaction.

The picture forwarded by Batich et al.[18] is essentially based on electronegativity considerations. However, trends in atomic electronegativity generally follow more closely those in ionization potentials than in electron affinities since the former are much larger. This is evident, for example, in the frequently employed definition (IP + EA)/2 for electronegativity. The interpretation presented in the present study indicates that geometry, and hence overlap change, is a more important factor in determining the relative orbital energies and accounts for the shifts in both the filled and unfilled b_1 orbitals of compounds II–V.

Conclusions

Electron transmission spectroscopy has been employed in the present study to determine the energies of those negative ion states of phosphabenzene, arsabenzene, and stibabenzene lying energetically above the ground states of the neutral molecules. We find that the mechanism put forward to explain the trends in the IP's was unable to account for those in the EA's. We believe that this is not an isolated example. In a recent study of the EA's of the fluoroethylenes,[20] it was also found that the factors invoked to describe variation of the IP's did not adequately account for those in the EA's. In this case the trends in the IP's had been explained in terms of resonance (mesomeric) and inductive interactions. However, a model focusing on geometry changes was able to explain the trends in both the IP's and the EA's. These illustrations indicate the importance of utilizing both sets of data for the interpretation of substituent effects and the complementary nature of photoelectron spectroscopy and ETS.

Acknowledgment. This research was supported in part by the Petroleum Research Fund, administered by the American Chemical Society (P.D.B.), Research Corporation (K.D.J.), and the National Science Foundation (A.J.A., P.D.B., and K.D.J.). We also wish to thank Dr. S. Staley and A. Howard for assistance with the synthesis of stibabenzene and Dr. N. S. Chiu for taking the pyridine spectrum. We are also grateful to Dr. J. Michl for valuable suggestions concerning the manuscript.

Registry No. I, 71-43-2; II, 110-86-1; III, 289-68-9; IV, 289-31-6; V, 289-75-8; VI, 289-52-1.

(18) Batich, C.; Heilbronner, E.; Hornung, V.; Ashe, A. J., III; Clark, D. T.; Cobley, U. T.; Kilcast, D.; Scanlan, I. *J. Am. Chem. Soc.* **1973**, *95*, 928. Bastide, J.; Heilbronner, E.; Maier, J. P.; Ashe, A. J., III *Tetrahedron Lett.* **1976**, 411.

(19) Ashe, A. J., III; Burger, F.; El-Sheik, M. Y.; Heilbronner, E.; Maier, J. P.; Muller, J. F. *Helv. Chim. Acta* **1976**, *59*, 1944.

(20) Chiu, N. S.; Burrow, P. D.; Jordan, K. D. *Chem. Phys. Lett.* **1979**, *68*, 121.